volumes at CT1 were larger than those at CT0, suggesting that tumor volumes increased during treatment planning. Changes in the tumor geometry during treatment are shown in Fig. 3 with the surface geometry maps. These maps show convex regions in red and concave regions in blue, allowing a visual understanding of the 3D tumor geometries. There are apparent differences in the distribution of red regions among the 6 patients before radiotherapy, showing that the deformation maps characterize the 3D shape of the tumors. In all 6 patients, the patterns of the colors did not change significantly during the treatment period even though the sizes of the tumors decreased dramatically. These results show that the six metastatic cervical lymph nodes shrank more or less evenly, maintaining the original characteristics of the 3D shape during the radiotherapy. Table 3 shows the image correlation coefficients between surface geometry maps constructed based on the CT images acquired before and during treatment. In all 6 patients, the maps obtained during treatment were strongly correlated statistically with the maps obtained before treatment; the average of the correlation coefficients in the six cases was 0.808 (range, 0.719–0.915).

Figure 4 shows the trajectories of the gravitational center of the tumors during treatment. Generally, the values of the displacement of the tumor centers were less than ±5 mm. In Patient 2, with the largest tumor volume before treatment and treated with conventional radiotherapy, the variation reached nearly 10 mm. Details of the tumor displacement during radiotherapy are shown in Table 4. The average displacement was 2.2 mm in the anterior–posterior (A–P) direction, 1.3 mm in the left–right (L–R) direction, and 2.2 mm in the superior–inferior (S–I) direction. The maximum displacement was 9.3 mm in the A–P direction (Patient 2), 4.1 mm in the L–R direction (Patients 2 and 4), and 9.1 mm in the S–I direction (Patient 2). For patients treated with IMRT, the average and maximum displacements were 1.9 and 5.1 mm in the A–P direction, 1.1 and 4.1 mm in the L–R direction, and 1.9 and 6.6 mm in the S–I direction.

DISCUSSION

The FE model and surface geometry maps with CT images were shown to be a useful tool to visualize the deformation of tumors during radiotherapy. Variations in the surface geometry map were also informative in indicating changes in tumor size, allowing the conclusion that surface geometry mapping can be a useful tool when comparing the effect of radiation among different tumor types, doses, and treatment types. It may be hypothesized that the surface geometry map may change unevenly if the distribution of cellular radiosensitivity, dose, or linear energy transfer, respectively, is heterogeneous in a tumor mass.

Table 3. Image correlation between surface geometry maps before and during treatment

	Correlation coefficient							
Patient	CT1	CT2	CT3	CT4	CT5	CT6	CT7	Average
1	0.927	0.856	0.642	0.777	0.760	0.817	0.787	0.795
2	0.841	0.717	0.678	0.678	0.682			0.719
3	0.887	0.882	0.729	0.797	0.739	0.824	0.810	0.810
4	0.916	0.904	0.923	0.807	0.720	0.734	0.792	0.828
5	0.922	0.851	0.941	0.917	0.931	0.931		0.915
6	0.874	0.839	0.703	0.729	0.804	0.771	0.767	0.784

Abbreviations: CT1 = CT images at 1 week; CT2 = CT images at 2 weeks, etc.

The 3D analysis of the target geometry using the surface geometry map showed that the six metastatic lymph nodes in this study shrank evenly, maintaining the original morphologic features throughout the treatment period. Image correlation analysis of the surface geometry maps showed that the maps obtained during treatment were strongly correlated with the initial map in all cases (overall average correlation coefficient, 0.808). The observation that tumors shrank uniformly throughout the treatment period was supported by quantitative analysis and by visual inspection. Uneven shrinkage of lymph nodes did not need to be considered in the radiotherapy of these patients. This means that changes in the 3D shapes of lymph nodes can be estimated by predicting the changes in volume, because the 3D shapes during the progress of the treatment can be obtained by shrinking the initial shape uniformly toward its center. This suggests that simulation methods that postulate even shrinkage of the tumor during radiotherapy can be applied as a tool to simplify the adaptive approach in IGRT. Elsewhere we have proposed the simulation method to predict changes in tumor volume during radiotherapy in cervical cancer (19). From those findings and also these, it is possible to postulate that the changes in the 3D shapes of lymph nodes during treatment—the deformation of metastatic lymph nodes—may be adjusted simply by interpolation or extrapolation from a comparison of CT images taken before and during radiotherapy.

Changes in target locations were almost all less than ±5 mm in the patients treated with IMRT; this is comparable to the setup errors in IMRT reported previously. Oita *et al.* analyzed the benefit of a real-time tumor-tracking radiotherapy setup in reducing setup errors (18). The results indicated that the range of displacement in a manual setup was about ±5 mm for the A–P, L–R, and S–I directions. In Patient 2, the change in target location reached nearly 10 mm. The reasons for the large change may have been related to the large size of the lymph nodes, patient immobilization, and the fusion process. This patient was immobilized using a thermoplastic mask without the three fiducial markers used in the other cases. The mask may not have completely prevented movement of the head and shoulders throughout the treatment. It is suggested that an accurate fusion process of the sequential images is essential to accurate analysis of the changes in the location of the tumor.

This study scanned patients with three fiducial markers. Because the markers are implanted into a rigid structure (mouthpiece), the position of each marker relative to the maxillary bone structure is stable, like a fixed marker to the bone, as also published previously (18). Each follow-up CT image

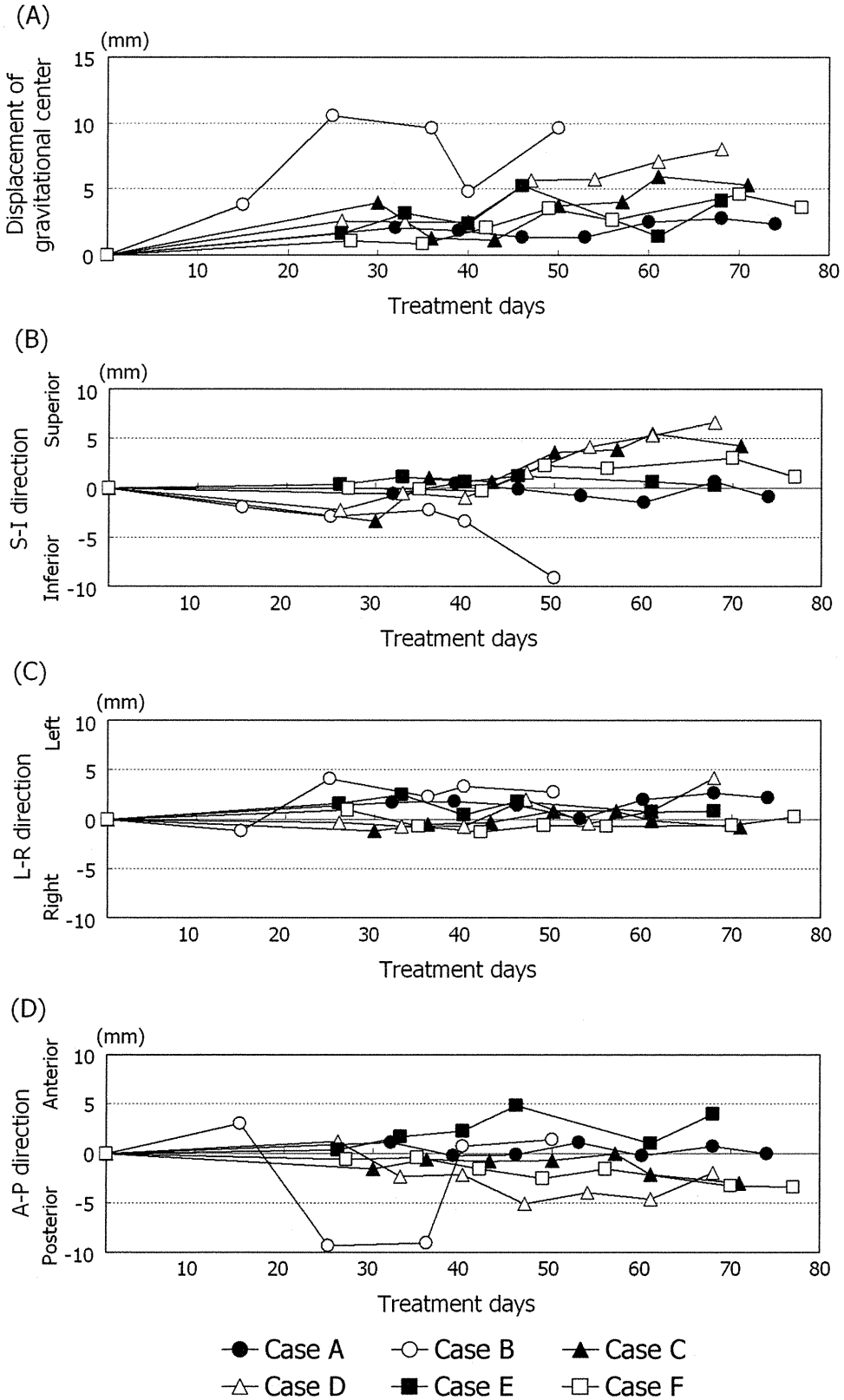

Fig. 4. Trajectories of the center of mass of the tumors during the course of treatment. (A) Overall displacement of the tumor. (B) Superior–inferior direction. (C) Left–right direction. (D) Anterior–posterior direction.

was shifted and rotated to fit the original CT image with reference to the location of these markers. By this process, the positions of the targets could be evaluated in the same coordinate system, without any effect by setup uncertainties. Thus, it was assumed that the effects of setup errors are negligible in this analysis and focus on the positional variations of the soft tissue caused by anatomic changes rather than setup errors. However, further study is required for a more

Table 4. Displacement of gravitational center of tumors in three directions during treatment

	A–P direction		L–R direction		S–I direction	
Patient	Average (mm)	Max (mm)	Average (mm)	Max (mm)	Average (mm)	Max (mm)
1	0.6	1.1	1.6	2.6	0.7	1.5
2	4.7	9.3	2.7	4.1	3.9	9.1
3	1.3	3.1	0.7	1.2	3.2	5.5
4	3.0	5.1	1.3	4.1	3.1	6.6
5	2.3	4.8	1.3	2.4	0.7	1.2
6	1.9	3.4	0.7	1.3	1.5	3.0
Total	2.2	9.3	1.3	4.1	2.2	9.1

Abbreviations: A–P = anterior–posterior; L–R = left–right; S–I = superior–inferior; Max = maximum.

accurate analysis to consider the possible bending of the cervical spine.

The CT scans for treatment planning are required to be acquired at a 2-mm slice width in our hospital. It would be advantageous to acquire all images with 2-mm thicknesses, but the weekly follow-up CT scans had to be made with a larger slice thickness because of limitations in imaging modalities. A slice thickness of the follow-up CT images during radiotherapy of 5 mm could lead to inaccuracies compared with 1- or 2-mm scans, especially in the S–I direction. By using a CT–CT fusion technique based on a mouthpiece with markers, the flexibility of the neck is not taken into account, and this flexibility influences the measurements of the location (center of gravity of the node).

CONCLUSION

The surface geometry map was useful in the accurate evaluation of the changes in volume and 3D shapes of the lymph nodes. The metastatic cervical lymph nodes in nasopharyngeal cancer patients were found to have decreased in size without significantly affecting the 3D morphologic features during radiotherapy. A surface geometry map based on the finite element model was shown to be useful in IGRT, particularly in the accurate recording and in the analysis of changes in tumor volumes and the 3D shape during radiotherapy.

REFERENCES

1. Barker JL Jr., Garden AS, Ang KK, *et al.* Quantification of volumetric and geometric changes occurring during fractionated radiotherapy for head-and-neck cancer using an integrated CT/Linear accelerator system. *Int J Radiat Oncol Biol Phys* 2004;59:960–970.
2. Li XA, Qi XS, Pitterle M, *et al.* Interfractional variations in patient setup and anatomic change assessed by daily computed tomography. *Int J Radiat Oncol Biol Phys* 2007;68:581–591.
3. Shirato H, Shimizu S, Kitamura K, *et al.* Organ motion in image-guided radiotherapy: Lessons from real-time tumor-tracking radiotherapy. *Int J Clin Oncol* 2007;12:8–16.
4. Riboldi M, Sharp GC, Baroni G, *et al.* Four-dimensional targeting error analysis in image-guided radiotherapy. *Phys Med Biol* 2009;54:5995–6008.
5. Den RB, Doemer A, Kubicek G, *et al.* Daily image guidance with cone-beam computed tomography for head-and-neck cancer intensity-modulated radiotherapy: A prospective study. *Int J Radiat Oncol Biol Phys 2009* 2010;76:1353–1359.
6. Wang J, Bai S, Chen N, *et al.* The clinical feasibility and effect of online cone beam computer tomography-guided intensity-modulated radiotherapy for nasopharyngeal cancer. *Radiother Oncol* 2009;90:221–227.
7. Houghton F, Benson RJ, Tudor GS, *et al.* An assessment of action levels in imaging strategies in head and neck cancer using TomoTherapy: Are our margins adequate in the absence of image guidance? *Clin Oncol* 2009;21:720–727.
8. Pawlowski JM, Yang ES, Malcolm AW, *et al.* Reduction of dose delivered to organs at risk in prostate cancer patients via image-guided radiation therapy. *Int J Radiat Oncol Biol Phys* 2010;76:924–934.
9. Varadhan R, Hui SK, Way S, *et al.* Assessing prostate, bladder and rectal doses during image guided radiation therapy: Need for plan adaptation? *J Appl Clin Med Phys* 2009;10:56–74.
10. Greene WH, Chelikani S, Purushothaman K, *et al.* Constrained non-rigid registration for use in image-guided adaptive radiotherapy. *Med Image Anal* 2009;13:809–817.
11. Hansen EK, Bucci MK, Quivey JM, *et al.* Repeat CT imaging and replanning during the course of IMRT for head-and-neck cancer. *Int J Radiat Oncol Biol Phys* 2006;64:355–362.
12. Smyth G, McCallum HM, Lambert EL, *et al.* A dose distribution overlay technique for image guidance during prostate radiotherapy. *Br J Radiol* 2008;81:890–896.
13. Ahunbay EE, Peng C, Godley A, *et al.* An on-line replanning method for head and neck adaptive radiotherapy. *Med Phys* 2009;36:4776–4790.
14. Wang H, Garden AS, Zhang L, *et al.* Performance evaluation of automatic anatomy segmentation algorithm on repeat or four-dimensional computed tomography images using deformable image registration method. *Int J Radiat Oncol Biol Phys* 2008;72:210–219.
15. Mohan R, Zhang X, Wang H, *et al.* Use of deformed intensity distributions for on-line modification of image-guided IMRT to account for interfractional anatomic changes. *Int J Radiat Oncol Biol Phys* 2005;61:1258–1266.
16. van Kranen S, van Beek S, Mencarelli A, *et al.* Correction strategies to manage deformations in head-and-neck radiotherapy. *Radiother Oncol* 2010;94:199–205.
17. Takao S, Tadano S, Taguchi H, *et al.* Analysis of three-dimensional characteristics in tumor morphology. *J Biomech Sci Eng* 2009;4:221–229.
18. Oita M, Ohmori K, Obinata K, *et al.* Uncertainty in treatment of head-and-neck tumors by use of intraoral mouthpiece and embedded fiducials. *Int J Radiat Oncol Biol Phys* 2006;64:1581–1588.
19. Takao S, Tadano S, Taguchi H, *et al.* Computer simulation of radiotherapy for malignant tumor: A mechanical analogy method. *J Biomech Sci Eng* 2009;4:576–588.